SUPPLEMENTAL INFORMATION

Table S1: CyCIF Antibody Information (Related to Figure 1)

Target Name	Source	Identifier
TTF1	Abcam	Clone EPR5955(2); Cat# ab206726; RRID: AB_2857980
B220 (CD45R)	ThermoFisher Scientific	Clone RA3-6B2; Cat# 41-0452-80; RRID: AB_2573598
CD45	BioLegend	Clone 30-F11; Cat# 103123; RRID: AB_493534
FOXP3	ThermoFisher Scientific	Clone FJK-16s; Cat# 11-5773-82; RRID: AB_465243
CD4	ThermoFisher Scientific	Clone 4SM95; Cat# 41-9766-82; RRID: AB_2573637
CD8α*	Cell Signaling Technology	Clone D4W2Z; Cat# 98941; RRID: AB_2756376
CD103**	R&D Systems	Clone Polyclonal; Cat# AF1990; RRID: AB_2128618
CD11c*	Cell Signaling Technology	Clone D1V9Y; Cat# 97585; RRID: AB_2800282
CD11b	Abcam	Clone EPR1344; Cat# ab204471; RRID: AB_2650514
Nkp46	R&D Systems	Clone Polyclonal; Cat# FAB2225F-025; RRID: AB_2149149
CD3e*	Cell Signaling Technology	Clone D4V8L; Cat# 99940; RRID: AB_2755035
Ki-67	Cell Signaling Technology	Clone D3B5; Cat# 12075; RRID: AB_2728830
PD-L1*	Cell Signaling Technology	Clone D5V3B; Cat# 64988; RRID: AB_2799672
PD-1	Cell Signaling Technology	Clone D7D5W; Cat# 61237; RRID: AB_2799604
Granzyme B*	Cell Signaling Technology	Clone E5V2L; Cat# 44153; RRID: AB_2857976
Perforin*	Cell Signaling Technology	Clone E3W4I; Cat# 31647; RRID: AB_2857978
TIM-3*	Cell Signaling Technology	Clone D3M9R; Cat# 83882; RRID: AB_2800033
Ly6G	eBioscience	Clone 1A8-Ly6G; Cat#: 12-9668-82; RRID: AB_2572720
TCF1	Cell Signaling Technology	Clone C63D9; Cat# 6709; RRID: AB_2797631
Vimentin	Cell Signaling Technology	Clone D21H3; Cat# 9854; RRID: AB_10829352
αSMA	Cell Signaling Technology	Clone D4K9N; Cat# 76113; RRID: AB_2857972
F4/80*	Cell Signaling Technology	Clone D2S9R; Cat# 70076; RRID: AB_2799771

Pan-Keratin	ThermoFisher Scientific	Clone AE1/AE3; Cat# 53-9003-82; RRID: AB_1834350
PCNA	Abcam	Clone PC10; Cat# ab201674; RRID: AB_2857977
CD4	R&D	Clone Polyclonal; Cat# FAB8165G; RRID: AB_2728839
CCR6	Abcam	Clone EPR22259; Cat# ab243852; RRID: AB_2860033
Granzyme B	Agilent Dako	Clone GrB-7; Cat# M7235; RRID: AB_2114697
TCF1	Cell Signaling Technology	Clone C63D9; Cat# 6444; RRID: AB_2797627
FOXP3	eBioscience	Clone 236A/E7; Cat# 41-4777-82; RRID: AB_2573609
CD8α	eBioscience	Clone AMC908; Cat# 50-0008-82; RRID: AB_2574149
PD-L1	Cell Signaling Technology	Clone E1L3N; Cat# 14123; RRID: AB_2798397
CD20	eBioscience	Clone L26; Cat# 50-0202-82; RRID: AB_11150959
TIM-3	Cell Signaling Technology	Clone D5D5R; Cat# 54669; RRID: AB_2799468
CD45	BioLegend	Clone HI30; Cat# 304008; RRID: AB_314396
PD-1	Abcam	Clone EPR4877(2); Cat# ab201825; RRID: AB_2728811
CD163	Abcam	Clone EPR14643-36; Cat# ab218293; RRID: AB_2889155
CD68	Cell Signaling Technology	Clone D4B9C; Cat# 79594; RRID: AB_2799935
Ki-67	Cell Signaling Technology	Clone D3B5; Cat# 12075; RRID: AB_2728830
HLA-DPB1	Abcam	Clone EPR11226; Cat# ab201527; RRID: AB_2890211
CD3D	Abcam	Clone EP4426; Cat# ab208514; RRID: AB_2728789
HLA A	Abcam	Clone EP1395Y; Cat# ab199837; RRID: AB_2728798
PCNA	Cell Signaling Technology	Clone PC10; Cat# 8580; RRID: AB_11178664
αSMA	Abcam	Clone EPR5368; Cat# ab202509; RRID: AB_2868435
Vimentin	Cell Signaling Technology	Clone D21H3; Cat# 9856; RRID: AB_10834530
CD16	Santa Cruz	Clone DJ130c; Cat# sc-20052 AF488; RRID: AB_2890161
Pan-Keratin	eBioscience	Clone AE1/AE3; Cat# 41-9003-82; RRID: AB_11218704
CD14	Abcam	Clone EPR3653; Cat# ab196169; RRID: AB_2890135
CD19	Abcam	Clone EPR5906; Cat# ab196468; RRID: AB_2889156
CD103	Abcam	Clone EPR4166(2); Cat# ab225153; RRID: AB_2884945

*Custom Conjugated Antibody from Cell Signaling Technology
**In-House Conjugated
See Star Methods for labeling details.

Figure S1

A

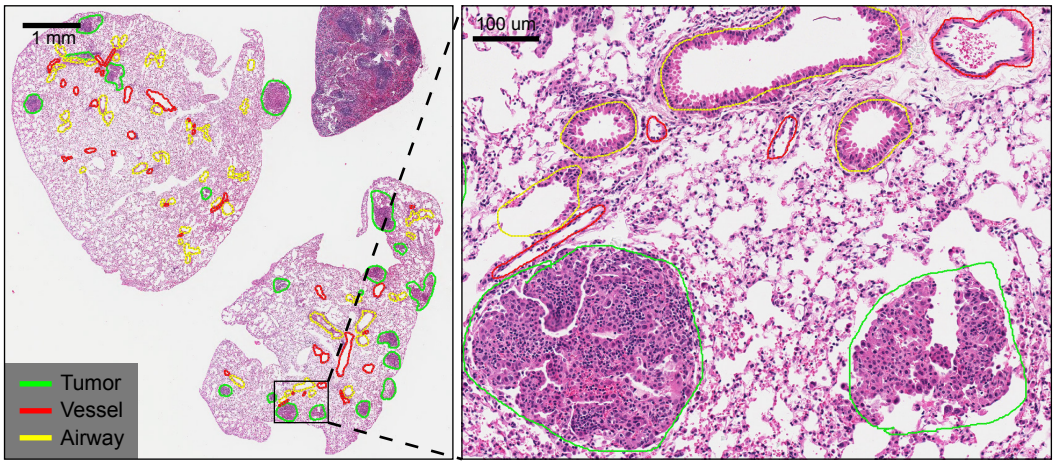

B

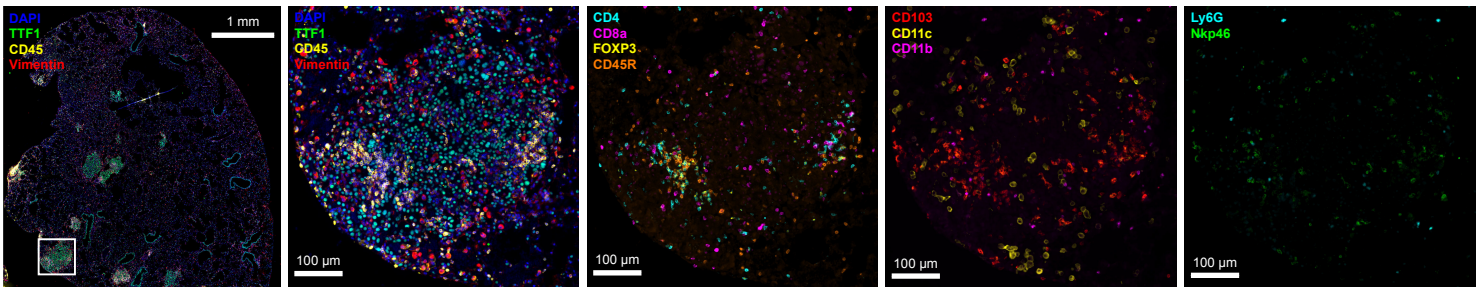

C

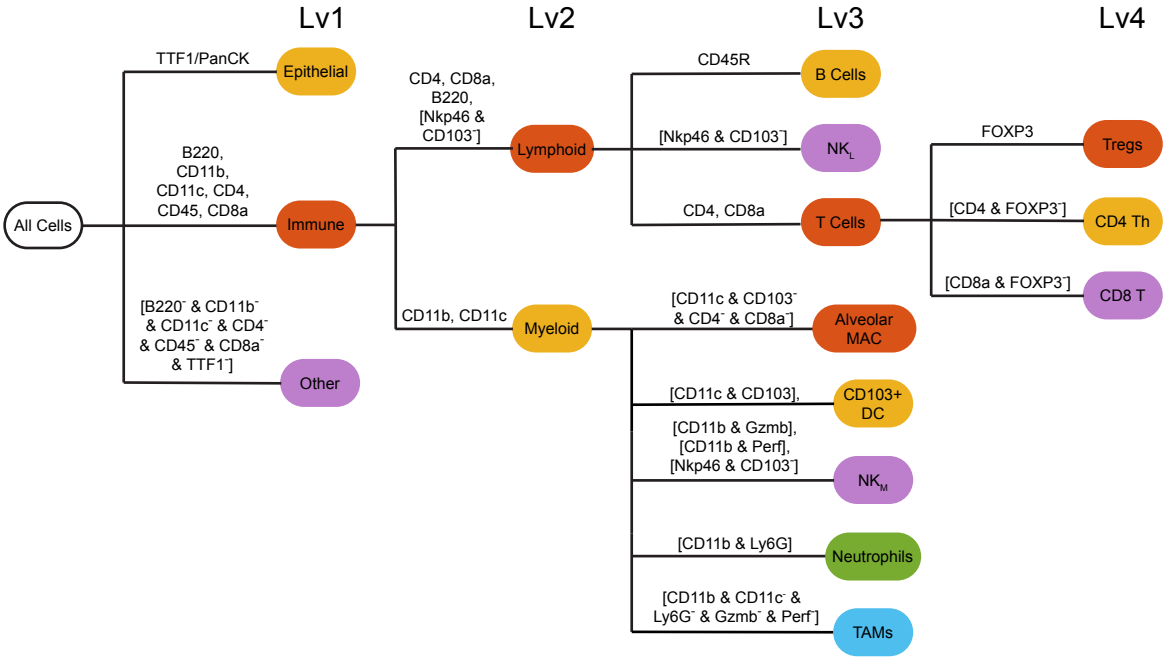

Figure S1. Multiplexed tissue imaging and cell type calling in the KP genetically engineered mouse model of cancer (Related to Figures 1 and 2)

(A) Representative image of H&E-stained section with pathology annotations indicated. Left, Scale bar: 1mm. Right, Scale bar: 100μm. (B) Representative multiplexed CyCIF images (whole lung lobe and single tumor inset) of tumor and immune markers from whole FFPE sections of KP LucOS tumor-bearing lung. Scalebar:1mm. Scalebar: 100 μm. Left, Scale bar: 1mm. Right, Scale bar: 100μm. (C) Cell type calling dendrogram for CyCIF image analysis; first immune, epithelial, and 'other' cell types were identified (Level 1, Lv1; shown in heat map of all cells), and then the immune cells were further clustered into lymphoid cells and myeloid cells (Level 2; Lv 2) and immune cell subtypes (Level 3 and Level 4; Lv3, Lv4: Treg, CD4 Th, CD8 Tc, B cells, NK cells (lymphoid marker-defined, 'NK-L'), alveolar macrophages, dendritic cells, NK cells (myeloid marker-defined, 'NK-M'), neutrophils, and tumor associated macrophages ($CD11b^{+}CD11c^{-}$).

Table S2: Mouse Experiment Information (Related to Figure 2-6)

Expt #	Mouse	Viral Construct	Sac Week	Treatment	# mice	Lobes	Tumors	Imaging modality
1	KrasLSL-G12D/+; Trp53fl/fl	Cre	8	none	5	10	531	CyCIF
1	KrasLSL-G12D/+; Trp53fl/fl	LucOS	8	none	5	10	107	CyCIF
1	KrasLSL-G12D/+; Trp53fl/fl	Cre+*Cxcl10a*	8	none	5	10	447	CyCIF
2	KrasLSL-G12D/+; Trp53fl/fl	Cre	8	none	5	8	599	RNAScope
2	KrasLSL-G12D/+; Trp53fl/fl	LucOS	8	none	5	8	113	RNAScope
2	KrasLSL-G12D/+; Trp53fl/fl	Cre+*Cxcl10a*	8	none	5	8	515	RNAScope
3	KrasLSL-G12D/+; Trp53fl/fl	LucOS	6	Ctrl 6 weeks	6	18	107	CyCIF
3	KrasLSL-G12D/+; Trp53fl/fl	LucOS	9	Ctrl 9 weeks	6	18	239	CyCIF
3	KrasLSL-G12D/+; Trp53fl/fl	LucOS	9	ICB 9 weeks	6	18	324	CyCIF
4	KrasLSL-G12D/+; Trp53fl/fl	LucOS	9	PBS (control)	7	14	198	CyCIF
4	KrasLSL-G12D/+; Trp53fl/fl	LucOS	9	Vax	8	16	201	CyCIF
5	Trp53fl/fl	Cre	4	none	3	3	0 (n/a)	CyCIF
5	Trp53fl/fl	LucOS	4	none	3	3	0 (n/a)	CyCIF
5	Trp53fl/fl	Cre	8	none	2	2	0 (n/a)	CyCIF
5	Trp53fl/fl	LucOS	8	none	3	3	0 (n/a)	CyCIF

Figure S2

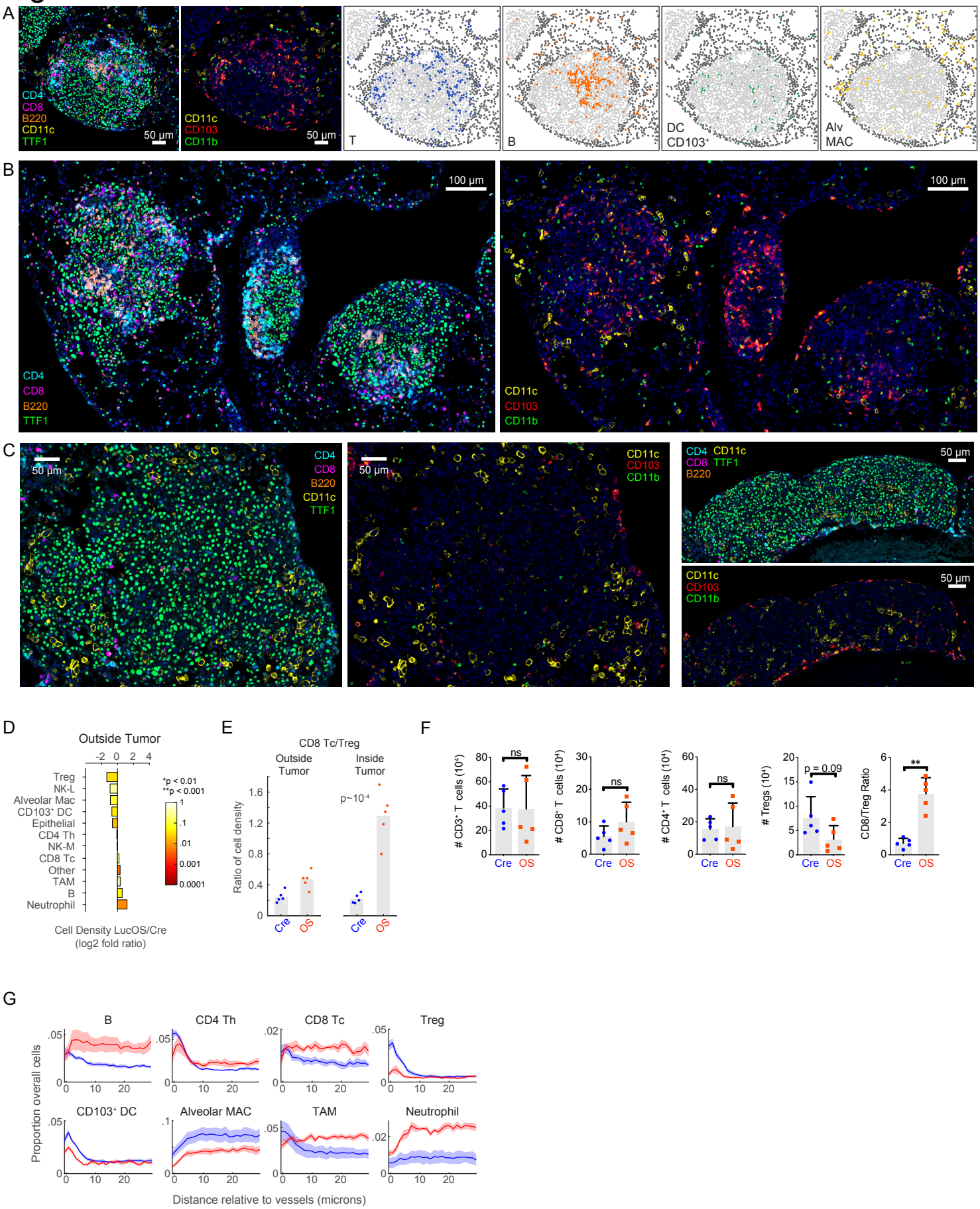
A
CD4
CD8
B220
CD11c
TTF1
50 μm
CD11c
CD103
CD11b
50 μm
T
B
DC
CD103+
Alv
MAC
B
100 μm
CD4
CD8
B220
TTF1
100 μm
CD11c
CD103
CD11b
C
50 μm
CD4
CD8
B220
CD11c
TTF1
50 μm
CD11c
CD103
CD11b
CD4 CD11c
CD8 TTF1
B220
50 μm
CD11c
CD103
CD11b
50 μm
D
Outside Tumor
-2 0 2 4
Treg
NK-L
Alveolar Mac
CD103+ DC
Epithelial
CD4 Th
NK-M
CD8 Tc
Other
TAM
B
Neutrophil
*p < 0.01
**p < 0.001
1
.1
.01
0.001
0.0001
Cell Density LucOS/Cre
(log2 fold ratio)
E
CD8 Tc/Treg
Outside Tumor
Inside Tumor
Ratio of cell density
1.6
1.2
0.8
0.4
0
p~10-4
Cre
OS
Cre
OS
F
CD3+ T cells (10⁴)
80
60
40
20
0
ns
Cre
OS
CD8+ T cells (10⁴)
30
20
10
0
ns
Cre
OS
CD4+ T cells (10⁴)
60
40
20
0
ns
Cre
OS
Tregs (10⁴)
20
15
10
5
0
p = 0.09
Cre
OS
CD8/Treg Ratio
6
4
2
0
**
Cre
OS
G
B
CD4 Th
CD8 Tc
Treg
CD103+ DC
Alveolar MAC
TAM
Neutrophil
Proportion overall cells
.05
.1
.02
0
10
20
Distance relative to vessels (microns)

Figure S2. Spatial analysis of immune cell-type composition in KP LucOS versus Cre tumor-bearing lung (Related to Figure 2)

(A) Representative CyCIF images of KP LucOS tumor shown in Figure 2B, showing co-expression patterns of myeloid markers CD11c, CD103, and CD11b. In the cell type dendrogram (Figure S1C) alveolar macrophages are defined as $CD11c^+$ cells that are negative for the conventional type 1 dendritic cell (cDC1) marker CD103 and having no appreciable expression of CD11b. The cDC1 population identified is $CD11c^+$ $CD11b^-$ $CD103^+$. The high level $CD11c^+$ $CD11b^+$ "myeloid" gate also captured $CD11b^+$ $CD11c^+$ conventional type 2 dendritic cells (cDC2), but this cell population could not be distinguished from $CD11b^+$ $CD11c^+$ tumor associated macrophages (TAMs), and, thus, was not described as an individual subset. Spatial maps of cell types (four plots on right) show that the $CD11c^+$ cells depicted in Figure 2B are alveolar macrophages and not dendritic cells. Alveolar macrophages express high levels of CD11c and are the most abundant myeloid population in the lung. Scale bar: 50μm. Additional representative CyCIF images of lymphocyte and myeloid markers are shown for (B) KP LucOS (Scale bar: 100μm) and (C) KP Cre (Scale bar: 50μm). (D) Log2 fold ratio of cell-type densities between LucOS and Cre in areas outside tumor (n = 5 mice/group, color: two tailed t-test p-value). (E) Ratio of CD8 Tc to Treg cell density measurements outside and inside of annotated tumor areas in LucOS versus Cre mice (n = 5 mice/group, bar = mean, two-tailed t-test). (F) T cell numbers in LucOS versus Cre mice calculated by flow cytometric analysis of dissociated tumor-bearing lung tissue (n = 5 mice/group, bar = mean, two-tailed t-test ns $p<0.1$). (G) Spatial frequency of indicated cell types relative to vessels (Cre and LucOS, n = 5 mice/group, mean +/- SEM).

Figure S3

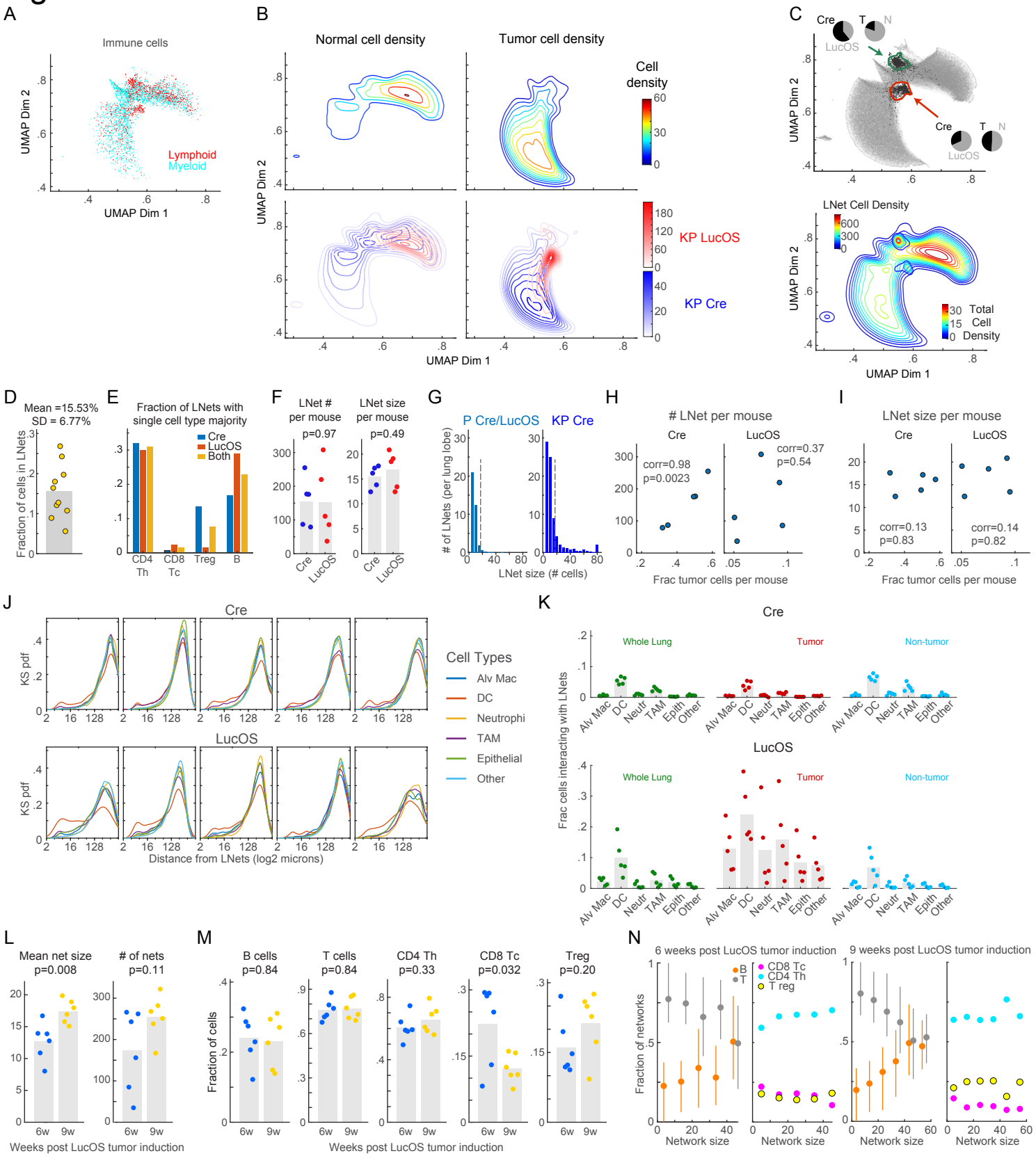
A
Immune cells
UMAP Dim 2
UMAP Dim 1
Lymphoid
Myeloid
B
Normal cell density
Tumor cell density
Cell density
KP LucOS
KP Cre
C
Cre
T
N
LucOS
LNet Cell Density
Total Cell Density
D
Mean =15.53%
SD = 6.77%
Fraction of cells in LNets
E
Fraction of LNets with single cell type majority
Cre
LucOS
Both
CD4 Th
CD8 Tc
Treg
B
F
LNet # per mouse
p=0.97
LNet size per mouse
p=0.49
G
P Cre/LucOS
KP Cre
# of LNets (per lung lobe)
LNet size (# cells)
H
# LNet per mouse
corr=0.98
p=0.0023
corr=0.37
p=0.54
Frac tumor cells per mouse
I
LNet size per mouse
corr=0.13
p=0.83
corr=0.14
p=0.82
J
Cre
LucOS
KS pdf
Distance from LNets (log2 microns)
Cell Types
Alv Mac
DC
Neutrophi
TAM
Epithelial
Other
K
Whole Lung
Tumor
Non-tumor
Frac cells interacting with LNets
L
Mean net size
p=0.008
# of nets
p=0.11
Weeks post LucOS tumor induction
M
B cells
p=0.84
T cells
p=0.84
CD4 Th
p=0.33
CD8 Tc
p=0.032
Treg
p=0.20
Fraction of cells
Weeks post LucOS tumor induction
N
6 weeks post LucOS tumor induction
9 weeks post LucOS tumor induction
B
T
CD8 Tc
CD4 Th
T reg
Fraction of networks
Network size

Figure S3. Characterization of lymphocyte networks (Related to Figure 3)

(A) Neighborhood embedding generated by the Visinity algorithm displaying all cells. (B) Density plots of normal and tumor cells in Visinity embedding of KP LucOS and KP Cre lung tissue. Color key represents relative cell density. (C) Visinity plots, black dots are cells in lymphonets. Arrows indicate Visinity cluster enriched in lymphonets, and pie charts summarize the composition and fraction of each cluster derived from LucOS and Cre and from tumor and normal tissues. (D) Plot of fraction of cells in lymphonets for LucOS and Cre together (n = 10 mice, 5 per group, bar = mean). (E) Fraction of lymphonets with indicated single-cell type majority for LucOS, Cre, and both combined (n = 5 mice per group). (F) Bar graph of lymphonet number (left) and size (right) in KP Cre versus KP LucOS mice (n = 5 mice/group, bar=mean, two-tailed t-test). (G) Histogram of number of lymphonets per lung lobe by lymphonet size for P fl/fl mice (treated with Cre and LucOS lentiviruses which do not induce tumors due to lack of Kras allele and harvested 4 or 8 weeks later; n = 11 mice and 11 lung lobes; see Table S4 for details) and KP Cre mice (n = 5 mice and 10 lobes). Dashed line placed for comparative reference. (H-I) Scatter plot of (H) number of lymphonets and (I) average size of lymphonets per Cre and LucOS by fraction of tumor cells per mouse (n = 5 mice/group, Pearson correlation and two-tailed p-value). (J) Kernel estimate probability density functions of distance of indicated cell populations from lymphonets in KP Cre and KP LucOS lung tissue (separate plots for each mouse analyzed; n = 5 mice/group). (K) Bar graphs of fraction of cells per cell type interacting with lymphonets for indicated cell populations in Cre and LucOS lung tissue (for whole lung area, tumor area, and non-tumor area, n = 5 mice/group, bar=mean). (L) Bar graphs of mean lymphonet size and lymphonet number and (M) immune cell composition in KP LucOS mice 6 weeks and 9 weeks after tumor induction (n = 6 mice/group, bar=mean, two-tailed t-test). (N) Lymphonet composition across network sizes. Left, B and T cells; right, T cell subtypes for KP LucOS mice 6 weeks and 9 weeks after tumor induction (n = 6 mice/group, mean +/- 25th percentile).

Figure S4

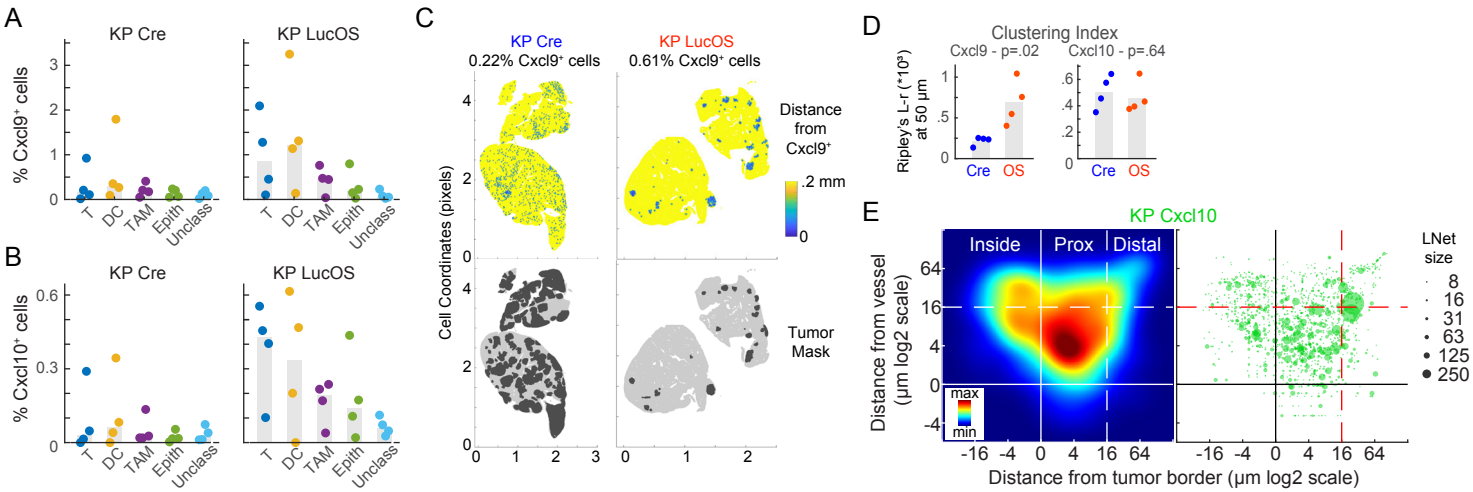
A
KP Cre
KP LucOS
% Cxcl9⁺ cells
T
DC
TAM
Epith
Unclass
B
KP Cre
KP LucOS
% Cxcl10⁺ cells
C
KP Cre
0.22% Cxcl9⁺ cells
KP LucOS
0.61% Cxcl9⁺ cells
Cell Coordinates (pixels)
Distance from Cxcl9⁺
.2 mm
0
Tumor Mask
D
Clustering Index
Cxcl9 - p=.02
Cxcl10 - p=.64
Ripley's L-r (*10³) at 50 µm
Cre
OS
E
KP Cxcl10
Inside
Prox
Distal
max
min
Distance from vessel (µm log2 scale)
Distance from tumor border (µm log2 scale)
LNet size
8
16
31
63
125
250

Figure S4. Spatial analysis of *Cxcl10* overexpression on lymphonets (Related to Figure 4)

(A) Bar plot of percent of *Cxcl9* expressing cells and *Cxcl10* expressing cells by cell type in KP Cre and KP LucOS lung tissues and (B) stacked bar graph showing fraction of positive cell per type in KP Cre and KP LucOS lung tissues (n = 4 mice/group mean +/- 25th percentile). 'DC' = CD103^{+} dendritic cells. (C) Map of all cells colored by distance to nearest *Cxcl9* mRNA positive cell measured by RNAScope™ *in situ* hybridization in KP Cre and KP LucOS lung tissue. (D) Spatial autocorrelation of *Cxcl9* and *Cxcl10* mRNA-expressing cells using Ripley's L function ('Ripley's clustering index') in KP Cre and KP LucOS mice (n = 4 mice/group, bar = mean). (E) Left, density plots of lymphonets by distance from closest blood vessel (y-axis) and tumor (x-axis) for KP *Cxcl10* cohort. Color key represents relative lymphonet density. Right, scatter plot lymphonets used to generate density plot (dot size represents the lymphonet size, n = 4 mice).

Figure S5

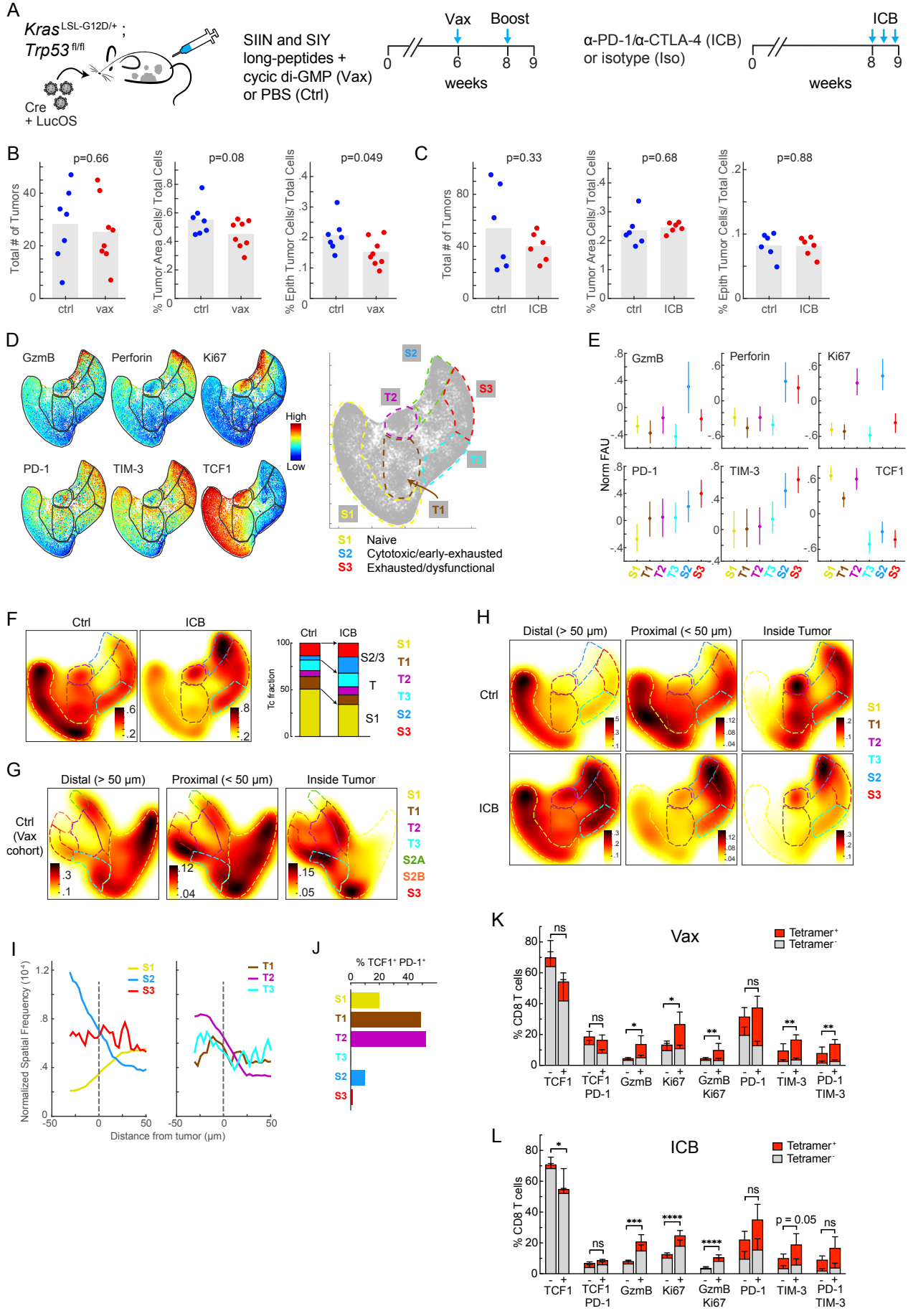
A
Kras LSL-G12D/+ ; Trp53 fl/fl
Cre + LucOS
SIIN and SIY long-peptides + cycic di-GMP (Vax) or PBS (Ctrl)
Vax
Boost
0
6
8
9
weeks
α-PD-1/α-CTLA-4 (ICB) or isotype (Iso)
ICB
0
8
9
weeks
B
p=0.66
p=0.08
p=0.049
Total # of Tumors
% Tumor Area Cells/ Total Cells
% Epith Tumor Cells/ Total Cells
ctrl
vax
C
p=0.33
p=0.68
p=0.88
Total # of Tumors
% Tumor Area Cells/ Total Cells
% Epith Tumor Cells/ Total Cells
ctrl
ICB
D
GzmB
Perforin
Ki67
PD-1
TIM-3
TCF1
High
Low
S1
S2
S3
T1
T2
T3
S1 Naive
S2 Cytotoxic/early-exhausted
S3 Exhausted/dysfunctional
E
GzmB
Perforin
Ki67
PD-1
TIM-3
TCF1
Norm FAU
S1 T1 T2 S2 S3
F
Ctrl
ICB
Tc fraction
S2/3
T
S1
S1 T1 T2 T3 S2 S3
G
Distal (> 50 µm)
Proximal (< 50 µm)
Inside Tumor
Ctrl (Vax cohort)
S1 T1 T2 T3 S2A S2B S3
H
Distal (> 50 µm)
Proximal (< 50 µm)
Inside Tumor
Ctrl
ICB
S1 T1 T2 T3 S2 S3
I
S1 S2 S3
T1 T2 T3
Normalized Spatial Frequency (10⁻⁴)
Distance from tumor (µm)
J
% TCF1⁺ PD-1⁺
S1 T1 T2 T3 S2 S3
K
Vax
Tetramer⁺
Tetramer⁻
% CD8 T cells
ns
*
**
TCF1
TCF1 PD-1
GzmB
Ki67
GzmB Ki67
PD-1
TIM-3
PD-1 TIM-3
L
ICB
Tetramer⁺
Tetramer⁻
% CD8 T cells
*
ns
***
****
p = 0.05
TCF1
TCF1 PD-1
GzmB
Ki67
GzmB Ki67
PD-1
TIM-3
PD-1 TIM-3

Figure S5. Multiparametric analysis of Tc functional states after anti-PD-1/anti-CTLA-4 immune checkpoint blockade (ICB) (Related to Figure 5)

(A) Schematic of treatment of KP LucOS mice with a SIIN and SIY long-peptide vaccine or anti-PD-1/anti-CTLA-4 immune checkpoint blockade therapy. (B) Bar graphs of total number of tumors (left), percent of tumor area cells (center), and percent epithelial cells (right) normalized by total cells for KP LucOS mice control (n = 7 mice) and with vax treatment (n = 8 mice). Vax treatment resulted in a significant reduction of tumor burden when immune cell infiltrate was excluded from tumor area calculations (bar=mean, two-tailed t-test). (C) Bar graphs of total number of tumors (left), percent of tumor area cells (center), and percent epithelial cells (right) normalized by total cells for KP LucOS mice control (n = 6 mice) and with immune checkpoint blockade (ICB) treatment (n = 6 mice, bar=mean, two-tailed t-test). (D) Palantir projection of CD8 Tc populations in KP LucOS mice treated with anti-PD-1/anti-CTLA-4 immune checkpoint blockade (ICB) or isotype control antibodies (Ctrl) (n = 10^4 cells sampled from n = 6 mice per treatment, see panel A for treatment schematic). The expression levels of the indicated markers are mapped to color (normalized between 0.1 and 99th percentile). Tc states defined by multiparameter measurements are indicated at the extremes of the representation (S1, S2, and S3) connected by transitional phenotypes (T1-T3) shown in the schematic to the right. (E) Plot of the normalized fluorescence units for each of the markers in the indicated Tc cell states and transitions (mean ± 25th percentile). (F) Heat map of Tc cell densities in Palantir projections for Ctrl and ICB groups (n = 10^4 cells per group). Right, stacked bar graph of the fraction of Tc cells in each state and transition. (G) Heat map of Tc cell densities in Palantir plots for KP LucOS following PBS treatment (Ctrl, vaccine cohort) separated by distance from tumor boundary (distal: >50 μm from the tumor boundary; proximal: <50 μm from the tumor boundary; and inside tumor, n = 10^4 cells). (H) Heat map of Tc densities in Palantir projections for KP LucOS mice following Ctrl or ICB treatment separated by distance from tumor boundary as in G (n = 10^4 cells per treatment). (I) Frequency of Tc cell states and transitions from tumor boundaries in ICB cohort. (J) Plot of the percent of Tc cells that are TCF1$^+$ PD-1$^+$ in each Tc cell state in ICB cohort. (K, L) Graph of flow cytometric analysis of dissociated tumor-bearing lung tissue from KP LucOS mice treated with Vax (K) or ICB (L) showing the percent of CD8

T cells expressing the indicated markers and the proportion of these populations that are SIIN and SIY peptide-MHC Tetramer+ versus Tetramer- (mean + SD, n = 5-7 mice per group; p-value *$p<0.05$, **$p<0.01$, ***$p<10^{-3}$, ****$p<10^{-4}$). Peptide-MHC tetramers do not fully capture low affinity TCR interactions, and some Tetramer negative cells analyzed may also be specific to the SIIN and SIY antigens.

Figure S6

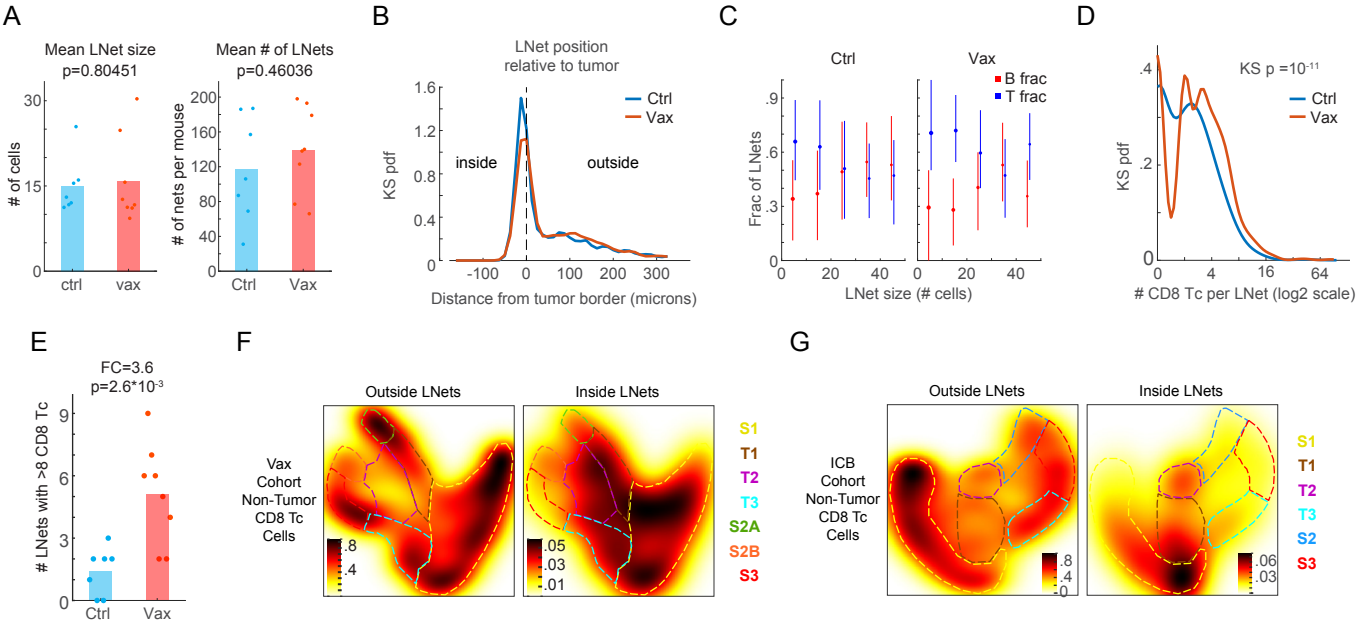
A
Mean LNet size
p=0.80451
# of cells
ctrl
vax
Mean # of LNets
p=0.46036
# of nets per mouse
Ctrl
Vax
B
LNet position
relative to tumor
KS pdf
Ctrl
Vax
inside
outside
Distance from tumor border (microns)
C
Ctrl
Vax
B frac
T frac
Frac of LNets
LNet size (# cells)
D
KS p =10-11
Ctrl
Vax
KS pdf
CD8 Tc per LNet (log2 scale)
E
FC=3.6
p=2.6*10-3
# LNets with >8 CD8 Tc
Ctrl
Vax
F
Outside LNets
Inside LNets
Vax
Cohort
Non-Tumor
CD8 Tc
Cells
S1
T1
T2
T3
S2A
S2B
S3
G
Outside LNets
Inside LNets
ICB
Cohort
Non-Tumor
CD8 Tc
Cells
S1
T1
T2
T3
S2
S3

Figure S6. Characterization of lymphonets after vaccine and immune checkpoint blockade immunotherapies (Related to Figure 6)

(A) Plot of the number of cells in lymphonets and the average number of lymphonets in KP LucOS mice without treatment (Ctrl) or treated with vaccination (Vax) (n = 7 and 8 mice, bar=mean, two-tailed t-test). (B) Kernel density probability density function of lymphonet spatial frequency relative to the tumor boundary for Ctrl (n = 7) and Vax (n = 8) mice. (C) Plot of the fraction of lymphonets comprised of T and B cells as a function of lymphonet size in Ctrl and Vax mice (mean +/- 25th percentile). (D) Kernel density probability density function of number of CD8 cytotoxic T cells per lymphonet for Ctrl (n = 7) and Vax (n = 8) mice (two-tailed KS test). (E) Bar graph of the number of lymphonets with >8 CD8 Tc cells in Ctrl (n = 7) and Vax (n = 8) mice (FC = fold change, two-tailed t-test) (F-G) Heat map of cell densities of non-tumor Tc cells present outside and inside lymphonets in Palantir projections for Vax (F, n = 14,480 and 978 cells) and ICB-treated (G, n = 13,948 and 735 cells) cohorts.

Table S3: Human samples information (Related to Figure 7)

Case	Age (yrs)	Sex	Pathology	AJCC 8th Edition Stage	Size (cm)	Side	Site	Histologic type	Grade	Treatment
1	68	F	Lung Adenocarcinoma	pT1b pNx	1.3	Right	Lower lobe	acinar predominant	G2: Moderately differentiated	None
2	56	F	Lung Adenocarcinoma	pT1cN2	2.3	Left	Upper lobe	solid predominant	G3: Poorly differentiated	None
3	60	M	Lung Adenocarcinoma	pT1bN0	1.4	Right	Lower lobe	acinar predominant	G3: Poorly differentiated	None
4	66	M	Lung Adenocarcinoma	pT2a pN0	2.2	Left	Upper lobe	acinar predominant	G2: Moderately differentiated	None
5	73	F	Lung Adenocarcinoma	pT2a pN0	2.2	Left	Upper lobe	solid predominant	G3: Poorly differentiated	None
6	73	F	Lung Adenocarcinoma	pT1a pN0	1	Right	Lower lobe	acinar predominant	G2: Moderately differentiated	None
7	73	M	Lung Adenocarcinoma	pT1cpN0	2.2	Left	Upper lobe	acinar predominant	G2: Moderately differentiated	None
8	63	F	Lung Adenocarcinoma	pT1bN0	1.2	Right	Upper lobe	papillary predominant	G2: Moderately differentiated	None
9	79	M	Lung Adenocarcinoma	pT2a pN0	2.1	Left	Upper lobe	acinar predominant	G2: Moderately differentiated	None
10	53	F	Lung Adenocarcinoma	pT3pN2	1.9	Right	Upper lobe	solid predominant	G3: Poorly differentiated	None
11	66	F	Lung Adenocarcinoma	pT1bN0	1.7	Right	Lower lobe	acinar predominant	G2: Moderately differentiated	None
12	66	F	Lung Adenocarcinoma	pT1bN0	1.3	Left	Lower lobe	papillary predominant	G2: Moderately differentiated	None
13	59	M	Lung Adenocarcinoma	PT3N0M1b	2	Right	Upper lobe	solid predominant	G3: Poorly differentiated	None
14	70	F	Lung Adenocarcinoma	PT1cN0	2.9	Right	Upper lobe	acinar predominant	G2: Moderately differentiated	None

Figure S7

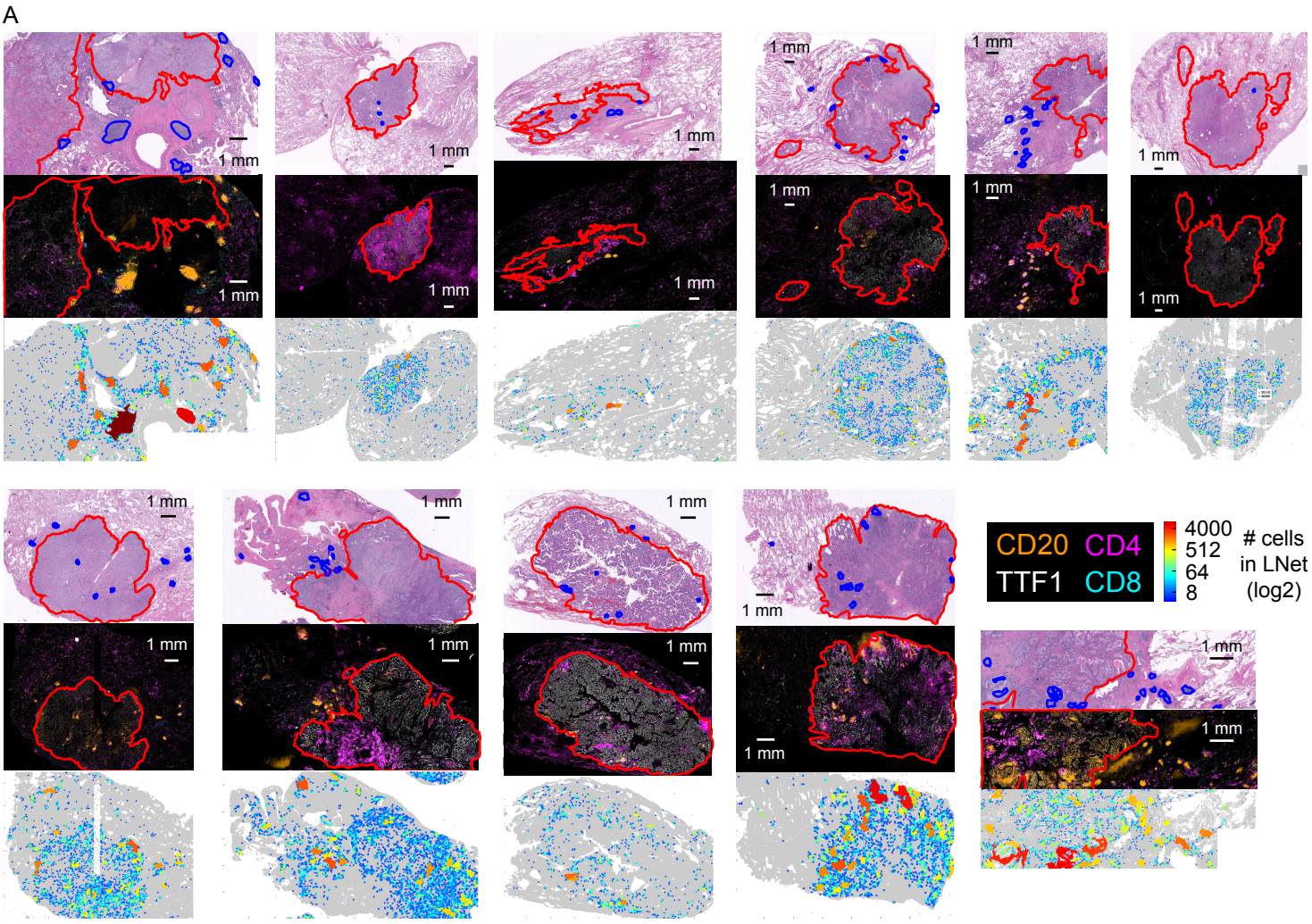
A
1 mm
CD20 CD4
TTF1 CD8
4000
512
64
8
cells in LNet (log2)

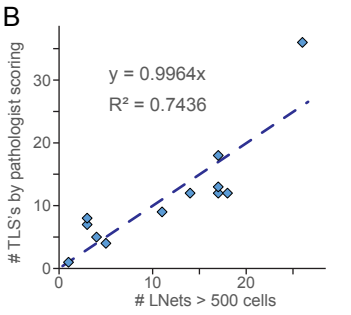
B
y = 0.9964x
R² = 0.7436
# TLS's by pathologist scoring
# LNets > 500 cells

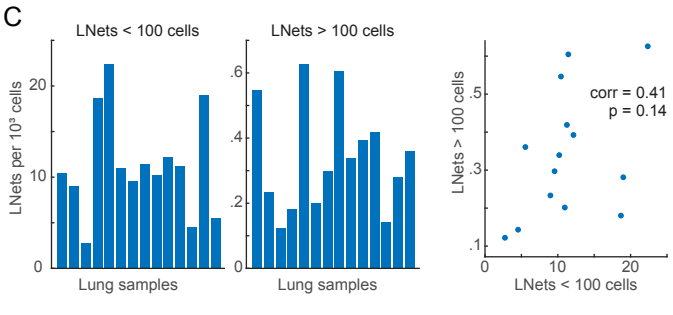
C
LNets < 100 cells
LNets > 100 cells
LNets per 10³ cells
Lung samples
LNets > 100 cells
LNets < 100 cells
corr = 0.41
p = 0.14

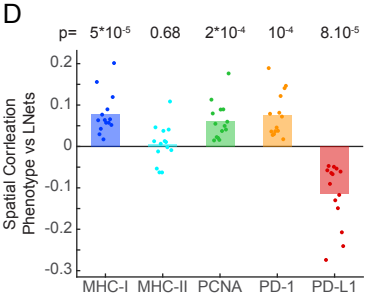
D
p= 5*10⁻⁵ 0.68 2*10⁻⁴ 10⁻⁴ 8.10⁻⁵
Spatial Correlation Phenotype vs LNets
MHC-I MHC-II PCNA PD-1 PD-L1

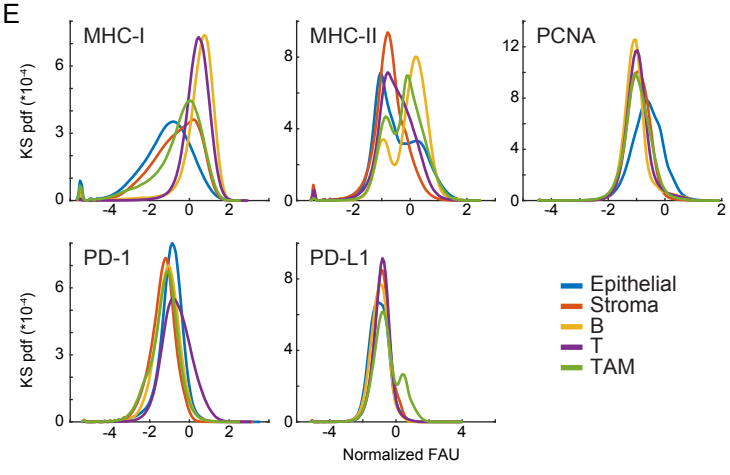
E
MHC-I
MHC-II
PCNA
PD-1
PD-L1
KS pdf (*10⁻⁴)
Normalized FAU
Epithelial
Stroma
B
T
TAM

Figure S7. Analysis of early-stage human lung adenocarcinoma (Related to Figure 7)

(A) Representative images of H&E and CyCIF images of human lung adenocarcinoma (Table S2; tumor areas outlined in red and lymphonets outlined in blue. Color map indicates lymphonet size. Scale bar: 1mm. (B) Scatter plot of number of TLS identified by pathology review versus number of large lymphonets (defined as >500 cells) in human lung tumor samples. Dashed lined linear regression from origin. (C) Bar graph and scatter plot of number of lymphonets per sample normalized by number of total cells in sample. Left, lymphonets <100 cells, right, lymphonets >100 cells. Pearson correlation and two-tailed test. (D) Spatial correlation of lymphocytes' likelihood of belonging to a lymphonet and the likelihood of myeloid cells expressing the indicated markers (n =1 4 samples, bar = mean, Pearson correlation and two-tailed test). (E) Kernel density probability density function of marker expression in indicated cell types.

Table S4: Lymphonets and Tertiary Structures in Human Lung Adenocarcinoma (Related to Figure 7)

	Lymphonet number by size					
CASE	**< 10 cells**	**11-30**	**31-64**	**65-500**	**>500**	**TLS (manual annotation)**
1	1168	642	112	112	36	n/a
2	1132	450	80	61	14	12
3	308	161	36	30	4	5
4	2385	988	109	69	3	7
5	2713	1232	219	152	17	12
6	1315	610	112	62	5	4
7	1100	537	124	95	1	1
8	1293	672	148	132	26	36
9	1184	584	118	83	17	18
10	1302	752	186	113	11	9
11	1260	679	143	100	18	12
12	502	279	59	41	3	8
13	2149	1180	202	86	17	13
14	580	366	74	75	18	40